Adhesion mechanisms of the mussel foot proteins mfp-1 and mfp-3

Qi Lin*, Delphine Gourdon*, Chengjun Sun†, Niels Holten-Andersen‡, Travers H. Anderson*, J. Herbert Waite†‡, and Jacob N. Israelachvili*‡§

Departments of *Chemical Engineering and †Molecular, Cellular and Developmental Biology, and ‡Graduate Program in Biomolecular Science and Engineering, University of California, Santa Barbara, CA 93106

Edited by George C. Schatz, Northwestern University, Evanston, IL, and approved January 3, 2007 (received for review September 7, 2006)

Mussels adhere to a variety of surfaces by depositing a highly specific ensemble of 3,4-dihydroxyphenyl-L-alanine (DOPA) containing proteins. The adhesive properties of *Mytilus edulis* foot proteins mfp-1 and mfp-3 were directly measured at the nano-scale by using a surface forces apparatus (SFA). An adhesion energy of order $W \approx 3 \times 10^{-4}$ J/m^2 was achieved when separating two smooth and chemically inert surfaces of mica (a common alumino-silicate clay mineral) bridged or "glued" by mfp-3. This energy corresponds to an approximate force per plaque of ≈100 gm, more than enough to hold a mussel in place if no peeling occurs. In contrast, no adhesion was detected between mica surfaces bridged by mfp-1. AFM imaging and SFA experiments showed that mfp-1 can adhere well to one mica surface, but is unable to then link to another (unless sheared), even after prolonged contact time or increased load (pressure). Although mechanistic explanations for the different behaviors are not yet possible, the results are consistent with the apparent function of the proteins, i.e., mfp-1 is disposed as a "protective" coating, and mfp-3 as the adhesive or "glue" that binds mussels to surfaces. The results suggest that the adhesion on mica is due to weak physical interactions rather than chemical bonding, and that the strong adhesion forces of plaques arise as a consequence of their geometry (e.g., their inability to be peeled off) rather than a high intrinsic surface or adhesion energy, *W*.

bioadhesion | *Mytilus edulis*

Marine mussels are experts at rapid, versatile, and permanent adhesion to solid surfaces in wave-swept seashores. This is a noteworthy achievement. Usually, the last few layers of water molecules adsorbed on hydrophilic surfaces are extremely difficult to remove, causing the failure of most man-made adhesives. Mussel adhesion is mediated by a holdfast structure known as the byssus, essentially a leathery bundle of threads tipped by flattened adhesive plaques that attach the mussel to a variety of hard surfaces (1). At least 12 proteins have been characterized from the byssus of *Mytilus* species, and eight of these are present in the adhesive plaque; three, however, are not limited to the plaque (Table 1). The collagens (preCol-D and -NG), for example, actually dominate the fibrous core of each byssal thread (2) and extend deep into the plaque matrix with their frayed ends (1). Another component, *Mytilus* foot protein-1 (mfp-1), is the major constituent of the protective cuticle covering all exposed portions of the byssus including the plaques (1, 3, 4). Although the masses of plaque proteins are variable, ranging from 5 kDa in mfp-3 to 240 kDa in preCol-D, all share basic isoelectric points (pI) and contain the posttranslationally modified amino acid, 3, 4-dihydroxyphenyl-L-alanine (DOPA).

The contact area between each plaque and a solid surface contains primarily mfp-3 and mfp-5 (12, 14, 15). Of all of the plaque proteins, these have the lowest mass and highest DOPA content at 15–30 mol% (Fig. 1). In contrast, mfp-1, the protein of the outer coating, has up to 15 mol% DOPA and a mass of ≈108 kDa. Previous studies of mussel adhesive proteins have proposed that the adhesion depends on DOPA (14, 16), and engineered synthetic analogs have generally confirmed that the higher the DOPA content, the stronger the adhesion (17–19). Whether stronger adhesion is the effect of redox chemistry (20, 21), metal coordination (22), or a combination of reactions remains unresolved (23). Recently, Lee *et al.* (24) measured an interaction energy of −22 kcal/mol between an atomic force microscope (AFM) cantilever tip functionalized with DOPA and a titanium oxide surface. The interaction was observed to be completely reversible and not subverted by the presence of water. Although exciting and insightful, these studies reduce mfps to a single functionality and ignore significant adhesive contributions made by the remainder of the DOPA-bearing protein/polymer backbone as well as the geometry of the attachment site (the plaque).

The present study explores and compares the adhesive behaviors of mfp-1 and mfp-3 on mica surfaces using the surface forces apparatus (SFA). Although the two proteins have roughly similar DOPA contents and pIs (≈10), they play functionally different roles in the byssus, namely, coating vs. adhesive. Both are observed or predicted to be flexible coils in solution (refs. 5 and 25, EXPASY "Protscale"), but there are striking differences in their primary sequences: mfp-1 has a faithfully repeated decapeptide consensus sequence with two posttranslational modifications besides DOPA: *trans*-4-hydroxyproline and *trans*-2,3-*cis*-3,4-dihydroxyproline (26). In contrast, mfp-3 shows no repeat patterns longer than 2 amino acids and contains uniquely modified 4-hydroxyarginine residues (6, 14).

The SFA measures the normal (attractive adhesion or repulsive) forces, $F_\perp$, as a function of surface separation, D, between two initially curved elastic surfaces, where the radius of curvature of the undeformed atomically smooth mica surfaces was typically $R \approx 1$ cm. Under a large compressive load $F_\perp$, the elastically deformed (flattened) contact diameter was typically 20–90 μm in the load range from 0.1 to 40 mN, corresponding to average pressures in the contact of 1–10 MPa (10–100 atm). These were the preloading pressures applied to the surfaces before they were separated to measure the adhesion. The adhesion forces were measured in buffer solution, first between two contacting mica surfaces bridged by either mfp-3 or mfp-1, then between an mfp-1-precoated surface and bare mica, as a function of the compression (preloading) pressure and shear.

The results reveal strikingly different behaviors in mfp-1 and mfp-3 and suggest that a strategic combination of primary sequence with DOPA functionalization may enable specification of polymers for coating or bridging functions.

Author contributions: Q.L., D.G., C.S., J.H.W., and J.N.I. designed research; Q.L., D.G., C.S., N.H.-A., and T.H.A. performed research; C.S. and N.H.-A. contributed new reagents/analytic tools; Q.L., D.G., and T.H.A. analyzed data; and Q.L., D.G., C.S., J.H.W., and J.N.I. wrote the paper.

The authors declare no conflict of interest.

This article is a PNAS direct submission.

Abbreviations: pI, isoelectric point; AFM, atomic force microscope; SFA, surface forces apparatus.

§To whom correspondence should be addressed. E-mail: jacob@engineering.ucsb.edu.

Table 1. Comparison of the DOPA-containing proteins in the adhesive plaques and threads of *Mytilus* species

Protein	Mass, kDa	pI	DOPA, mol%	Location	Ref.
mfp-1	108	10	10–15	Cuticle	5, 6
mfp-2	45	9	5	Plaque	7, 8
mfp-3	5–7	8–10	10–20	Plaque	9
mfp-4	90	10.5	2	Plaque	10
mfp-5	9	9–10	30	Plaque	11
mfp-6	11	10	2	Plaque	12
preColD	240	9	<1	Thread, plaque	13
preColNG	240	9	<1	Thread, plaque	2

Results for mfp-6 are for *M. californianus*; all others are for *M. edulis*.

Results

Mussel Plaques Adhere Well to Mica. Mussels can stick to a wide variety of surfaces, such as mineral, paraffin, Teflon, steel, glass, tooth, bone, hydrophilic, and hydrophobic, smooth, and rough. Unlike many materials, mica is a hard, inert material well known for its atomically smooth surface (often used in AFM and SFA studies). To confirm that mussels can actually attach to mica, a macroscopic experiment was first carried out in a mariculture system: Two big, freshly cleaved mica sheets were put into an aquarium tank through which fresh sea water was passed continuously. Three different species of mussel, *Mytilus galloprovincialis*, *Mytilus californianus*, and *Perna canaliculus*, were loosely hung next to the mica sheets with rubber bands. As shown in Fig. 2*a*, all of the mussels attached threads overnight to the nearby mica surfaces. Fig. 2*b* is a closer look at the third mussel from the top, which had spread threads on two mica sheets and which was able to carry the weights of three mussels and the bottom mica sheet using only three threads, indicative of strong adhesion.

AFM imaging further confirmed that the mussel foot protein adsorbs to the mica surface: Fig. 3 shows tapping mode AFM images of an mfp-1-coated mica surface. Before imaging in air, three droplets of mfp-1 solution (pH 5.5) were placed on a freshly cleaved mica surface for 30 s, then rinsed several times in buffer solution to remove excess proteins and then blow-dried thoroughly with dry nitrogen gas. The flat plateau regions P in Fig. 3 are ≈1 nm above the flat (mica) surface, which gives the thickness of the dehydrated protein layer on mica.

Measurement of mfp Adhesion at the Nano Scale. Force-distance profiles and adhesion forces were measured to test the ability of mfp to "glue" two mica surfaces together. After the mica surfaces were brought into flat adhesive contact in air (Fig. 4*a*), three droplets of mfp solution were injected between the surfaces from the side of the junction (Fig. 4 *a* → *b*). The apparatus was well sealed during the entire experiment except when pure nitrogen gas was passed through the chamber during protein injections to avoid contamination from the outside air. After the system reached thermal equilibrium, which usually takes ≈30 min, the surfaces were separated very slowly (quasistatically) at a constant separation velocity of ≈20 Å/s. Fig. 4 *b* → *c* shows the deformations and adhesion measured on separating the two surfaces bridged by mfp-3: the surfaces jumped apart abruptly (within 0.5 s) from D = 30 to 160 Å (Fig. 5). This adhesion indicates that the molecules adsorb to both surfaces at the edge of the junction (Fig. 4*b*), acting as short (≪10 nm) adhesive bridging tethers when the surfaces are separated (Fig. 4*c*).

Successive force runs were carried out after the first jump out from adhesive contact. In these, the surfaces were slowly (≈20 Å/s) brought back into contact (Fig. 6, open symbols). No adhesive jumps into contact were observed. Subsequent adhesive jump-outs showed that the adhesion is not a fixed value, and can be increased with the contact time and/or load, but it never exceeds the strength at the first separation (Fig. 6 *Inset*).

The same sequence of experiments was repeated on the mfp-1 system, for which no initial adhesion was ever measured. The possibility of long-range bridging forces was excluded because no attractive forces were measured at separations beyond those shown in the figures (≈100 nm), and out to 1,000 nm, which is longer than twice the contour length (≈380 nm) of an mfp-1 molecule (twice the length being the range where fully extended molecules on each surface could, in principle, bridge). In this case, neither a prolonged contact time nor higher compressive loads could induce any adhesion. The forces on successive approaches and separations (not shown) were identical to the force profile for mfp-1 shown in Fig. 5.

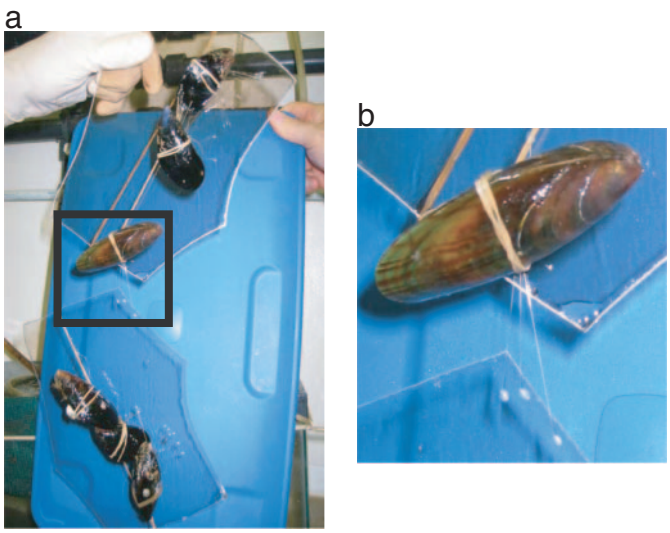

Fig. 2. Mussels on mica. (*a*) All three mussel species adhered to mica. (*b*) Enlargement of square area in *a* showing the mussel with byssal threads connected to both mica sheet and bearing the weight of a mica sheet with three congeners by means of only three byssal threads.

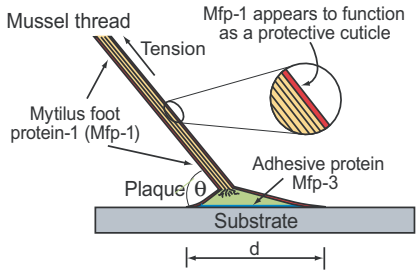

Fig. 1. Schematic drawing of a byssal thread attached to a substrate.

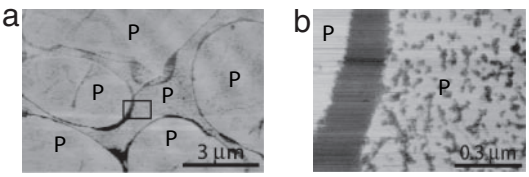

Fig. 3. AFM of mfp-1 adsorbed on mica. (*a*) Tapping mode AFM image of a mfp-1 coated mica surface after drying. (*b*) Magnified rectangular area in *a* showing ≈1-nm-thick flat layers (light patches, P) on the bare mica (dark areas). The bare mica regions are likely due to shrinking upon dehydration of the mfp-1 layer during drying.

BIOPHYSICS

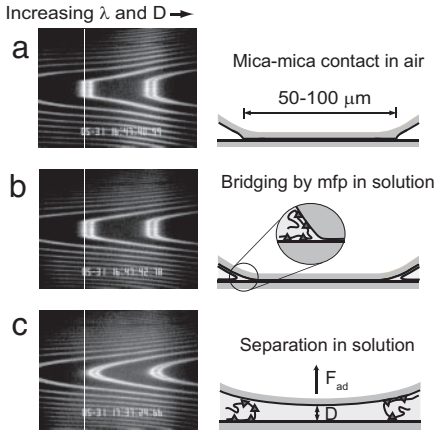

Fig. 4. Two mica surfaces bridged by mfp-3. (*Left*) Fringes of equal chromatic order (FECO) images during an mfp-3 bridging experiment. (*Right*) Schematic drawings of corresponding molecular processes occurring at the junction. Triangles represent the likely binding sites on the molecules. (*a*) Two mica surfaces in flat adhesive contact in air. (*b*) Same surfaces after an mfp solution was injected between them. (*c*) A configuration of surfaces immediately after the jump out from adhesive contact. The white vertical line indicates the original wavelength, λ, of mica–mica contact (corresponding to $D = 0$).

These studies were conducted at acidic pH (pH 5.5) to prevent DOPA oxidation to reactive quinones and are not inconsistent with mussel byssus. A recent mass spectrometric analysis of plaque footprints reported that DOPA in mfp-3 is maintained in reduced form even after 24 h of direct exposure to seawater (pH 8.2) (15). Such redox stability for DOPA would never have occurred with purified mfps in seawater. An additional bridging experiment for mfp-1 in pH 7.0 buffer was conducted for comparison. To avoid DOPA oxidation before deposition, three droplets of mfp-1 solution (in pH 5.5 buffer) were first injected between the two surfaces. Afterward, the chamber was flushed

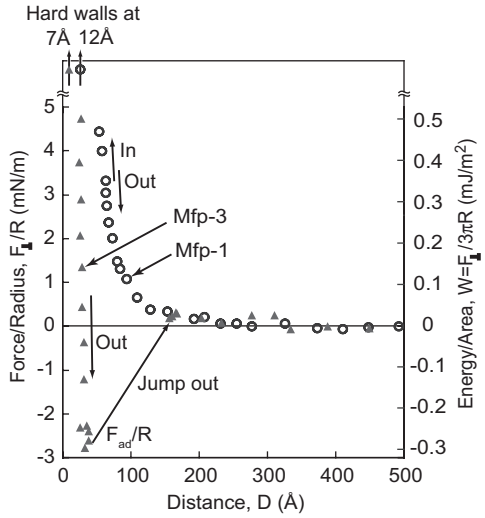

Fig. 5. Normal forces, $F_\perp$, measured on separating two mica surfaces (Out curves) as a function of surface separation, D, in solutions of mfp-1 (open circles) and mfp-3 (filled triangles). The left ordinate gives the measured *force*, $F_\perp/R$ (normalized by the radius of the surfaces, R). The right ordinate gives the corresponding adhesion *energy* per unit area, W, between two flat surfaces, defined by $W = F_\perp/3\pi R$ (27). Attractive adhesion forces were measured only in solutions of mfp-3, whereas the forces were always repulsive and reversible upon approach in solutions of mfp-1. Also, note that the repulsive ''hard walls'' for mfp-1 films were always farther out than for mfp-3 films.

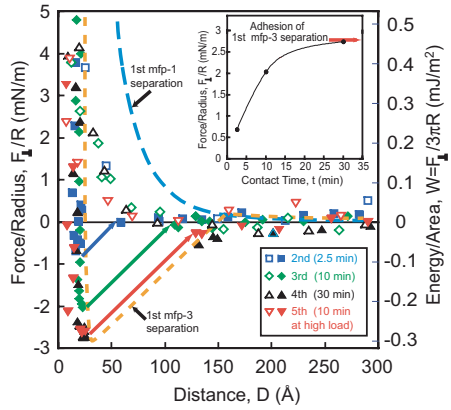

Fig. 6. Successive force runs measured between mica surfaces bridged by mfp-3 after the first separation. Open symbols are the forces on approach; filled symbols are the forces on separation after different compressive loads and/or various contact times. The dashed lines show the bridging force curves of Fig. 5. (*Inset*) Adhesion vs. contact time; the horizontal arrow shows the adhesion value of the first separation.

with pH 7.0 buffer solution with the surfaces in contact. No adhesion was measured, and the force-distance profiles (not shown) were similar to those at pH 5.5.

Experiments at even higher pH, such as the pH of the seawater (8.2) or the pIs of mfp-1 (pH~10) and mfp-3 (pH 8~10) are, of course, possible; however, the results may not be meaningful because mfp-1 and mfp-3 form discolored precipitates at pH 7.5–8.5.

Shearing Forces. Because neither a prolonged contact time nor high compressive loads could induce any adhesion in the mfp-1 system, the effect of shear was also investigated. Three droplets of mfp-1 solution (pH 5.5) were put on a freshly cleaved mica surface for 10 s, then rinsed thoroughly with buffer solution to remove excess protein. At the end of each rinse, a large drop of buffer solution was left on the protein-coated surface to keep it wet, which would then be mounted into the SFA chamber together with another (bare) mica surface. The two surfaces were then brought together until the droplet bridged the two surfaces. After the system had reached thermal equilibrium (≈30 min), the surfaces were moved toward each other at a constant velocity of ≈20 Å/s, and after contact for a certain time, separated. Again, no adhesive jumps were observed either on approach or separation (Fig. 7), and again, neither a prolonged

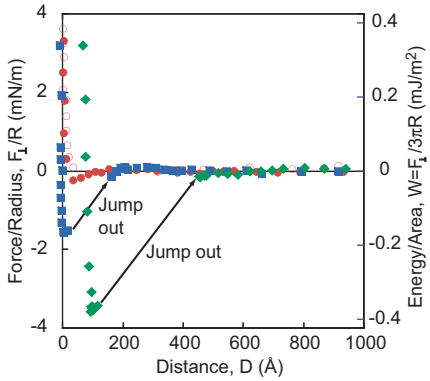

Fig. 7. Measured normal forces, $F_\perp$, as a function of surface separation, D, between an mfp-1-coated mica surface and a bare mica surface in buffer solution before (circles) and after (squares and diamonds) shearing. Open symbols are the forces on approach; filled symbols are the forces on separation.

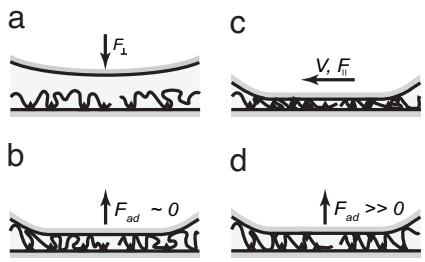

Fig. 8. Schematic drawing of the interactions and rearrangements between a protein adsorbed on a mica surface and a bare mica surface under compression (*a*), separation without shear (*b*), shear without separation (*c*), and separation after shear (*d*). Triangles represent the binding sites on the protein molecules.

contact time nor a high load could induce adhesion. These results indicate that all of the binding sites of mfp-1 adhere to the mica surface once they come into contact with it, leaving no free or exposed sites to attach to a second surface.

However, a finite adhesion was observed after shearing (Fig. 7). Prolonged shearing, either in distance or time, increased the adhesion. Fig. 8 shows a schematic drawing of a possible explanation for this shear-induced adhesion. It is suggested that some of the binding sites on the proteins, most of which are initially attached to one surface only, become rearranged by the shearing force, and start to attach to the opposite surface. The longer distance and/or time of shearing, the more molecules and binding sites are affected, leading to the increased adhesion.

Discussion and Conclusions

Implication of the Adhesion Energy, *W*. Mussel foot proteins, especially mfp-3, can adhere to mica surfaces with an adhesion energy of at least $W \approx 0.3$ mJ/m^2, as shown in Figs. 5 and 6 (adhesion energies up to two times stronger were measured at higher protein concentrations; data not shown). For a plaque of diameter $d \approx 3$ mm (see Fig. 1) and area $A = \pi(d/2)^2 \approx 10^{-5}$ m^2, having an adhesion energy with a surface of $W \approx 0.3$ mJ/m^2 = 3×10^{-4} J/m^2 extending over a distance of $\delta \approx 30$ Å $= 3 \times 10^{-9}$ m (the effective bridging bond length as found in Fig. 5), when separated from the surface in the normal direction, the adhesion force will be

$$F_{\text{ad}} = WA/\delta \approx 1\,N, \qquad [1]$$

or ≈100 gm per plaque.

Thus, the relatively weak surface adhesion energy we measured, of the order of $W \approx 3 \times 10^{-4}$ J/m^2, nevertheless corresponds to a very significant *force* per plaque of order 100 gm, more than enough to hold a mussel in place under almost any conditions. However, to ensure this high adhesion force, two apparent conditions must be satisfied:

1. The plaque must not be able to *peel* away, say from one end to the other, otherwise the plaque's adhesion force would not be given by Eq. **1** but by Eq. **2** (28)

$$F_{\text{ad}} = WA/d, \qquad [2]$$

and because $d \gg \delta$, this would correspond to a very low adhesion force, about a factor of 3 mm/3 nm $\approx 10^6$ lower! The geometry of the plaque (Fig. 1) apparently ensures that it cannot be detached by peeling from the outer rim.

2. Multiple threads at angles θ between 0 and 90° to the substrate and to each other, like a tripod, further ensure that the mussel cannot be easily dislodged, one plaque at a time, by peeling or shear forces, because the multiple contacts do not allow for θ to vary much, thus ensuring high adhesion and friction. A similar situation arises with the thread-like gecko spatulas at the foot pads of geckos that are responsible for their high adhesion and friction, especially at spatula angles θ of 20–30° (29). In the case of mussels, typical θ angles for unstrained threads of ≈20° have been reported (30), although θ can reach 50° for mussels pulled in the normal direction, and decrease to 15° when pulled (sheared) horizontally to the surfaces.

Successive force runs with mfp-3 after the initial bridging separation showed the adhesion to be nonpermanent, but it could be partially restored after prolonged contact times and/or higher loads. This finding indicates that the adhesion on mica is consistent with physical interactions, such as electrostatic and H bonds, rather than to the chemical bonding[¶] observed on more reactive surfaces (24). Our results for mfp-1 and mfp-3 on mica are consistent with the coating and adhesive functions attributed to these proteins. The adhesion mechanism proposed for mica may not be representative of mfp-1 and mfp-3 on all surfaces, although we may note that mica is an ion-exchangeable silicate material, similar to many other clay surfaces.

Functionalities of mfp-1 and mfp-3. The AFM imaging and SFA experiments show that mfp-1 can adhere well to one mica surface, but is unable to link to another (unless sheared). Parameters such as contact time and contact pressure were investigated and found to have little effect under static loading/contact condition. These results are consistent with the nature of the mussel foot protein molecules: Mfp-1 is a large molecule (108 kDa) with 80 regular repeat units that contain 10–15 mol% DOPA, whereas mfp-3 is much smaller (only 5–7 kDa) with no repeat units, which allows variants to form different structures, and contains 10–20 mol% DOPA. Although both mfp-1 and mfp-3 can adhere to mica by forming hydrogen bonds by DOPA and other hydroxylated amino acids, at a narrow junction the small mfp-3 would be better able to (*i*) diffuse into the gap and (*ii*) form more binding sites because of its higher mobility and flexibility. Mfp-1 is likely to adsorb on a single surface with its unbound segments facing out to protect the surface. This "protective" rather than "adhesive" protein layer cannot be removed/squeezed out by hard or frequent compression/separations.

Our results also show that shearing two surfaces with a layer of mfp-1 between them can significantly alter (increase) the adhesion, without damaging the surfaces even after several shearing cycles. The shearing apparently forces some of the already bound proteins or sites to detach and bind to the opposite surface. There are two possible explanations for this: shear-dependent conformational change and degradation. Shear-dependent conformational changes in integrin improve its binding to collagen (31), and the shear induced degradation of biopolymers into smaller fragments is well known, for example, shear fragmentation of DNA (32). Together, the results suggest that mfp-1 behaves as a protective coating and that mfp-3 is the real adhesive protein, acting like a "glue" for the mussels' binding onto surfaces. This measurable distinction is noteworthy, because it is increasingly argued that the presence of DOPA will categorically enhance adhesion (20, 21). In reality, although the presence of DOPA in proteins may ensure good adsorptive or cohesive properties, its effectiveness as an adhesive may be determined by additional factors such as the protein conformation (for determining selectivity), and the geometry and dispo-

[¶]Mica is chemically very inert and undergoes no known chemical reactions unless the outermost layer of the siloxane Si–O–Si group is first broken by, for example, plasma etching. These bonds are not even affected by hydrofluoric acid. However, the surface energy of mica in the crystal is extremely high, of the order of 3,000 mJ/m^2, due to the strong potassium-mediated ionic bonds, which are directional but not covalent, that bridge the negatively charged oxygen atoms on the two opposing basal lattice planes.

sition of the attachment sites (plaques) for determining the ultimate adhesive strength of the byssus.

Materials

Mussel foot proteins mfp-1 and mfp-3 were purified by the authors according to published procedures with feet obtained from commercially shucked mussels *Mytilus edulis* (Northeast Transport, Waldoboro, ME) and flash-frozen in liquid N_2 (33). The mol% content of DOPA, which is used as a measure of purity, was ≈12 mol% for samples of mfp-1 and ≈16 mol% for mfp-3 as determined by amino acid analysis after complete hydrolysis (34). Sample purity was also confirmed by polyacrylamide gel electrophoresis and MALDI-TOF. Purified samples were freeze-dried and stored at −80°C. After suspending in pH 5.5 buffer solution, which contained 0.1 M acetic acid, sodium acetate (EMD Chemicals, Gibbstown, NJ), and 0.25 M potassium nitrate (Aldrich, St. Louis, MO), the protein solutions were divided into aliquots and stored in aluminum foil-covered vials at 4°C before experiments. This acidic pH and light-free condition was necessary for reducing DOPA oxidation in solution (33), and the high salt concentration provides a similar saline level as in seawater. Milli-Q water (Millipore, Bedford, MA) was used for all of the cleaning and solution-making.

This work was supported by the Institute for Collaborative Biotechnologies (ICB) of the University of California (Santa Barbara) through U.S. Army Research Office Contract DAAD19-03-D-0004, National Institutes of Health Grant DE 015415, and National Aeronautics and Space Administration University Research Engineering and Technology Institute (NCC-1-02037).

1. Waite JH, Andersen NH, Jewhurst S, Sun CJ (2005) *J Adhes* 81:297–317.
2. Waite JH, Qin XX, Coyne KJ (1998) *Matrix Biol* 17:93–106.
3. Benedict CV, Waite JH (1986) *J Morphol* 189:171–181.
4. Sun CJ, Waite JH (2005) *J Biol Chem* 280:39332–39336.
5. Deacon MP, Davis SS, Waite JH, Harding SE (1998) *Biochemistry* 37:14108–14112.
6. Waite JH, Housley TJ, Tanzer ML (1985) *Biochemistry* 24:5010–5014.
7. Inoue K, Takeuchi Y, Miki D, Odo S (1995) *J Biol Chem* 270:6698–6701.
8. Rzepecki LM, Hansen KM, Waite JH (1992) *Biol Bull* 183:123–137.
9. Papov VV, Diamond TV, Biemann K, Waite JH (1995) *J Biol Chem* 270:20183–20192.
10. Zhao H, Waite JH (2006) *Biochemistry* 45:14223–14231.
11. Waite JH, Qin XX (2001) *Biochemistry* 40:2887–2893.
12. Zhao H, Waite JH (2006) *J Biol Chem* 281:26150–26158.
13. Qin XX, Coyne KJ, Waite JH (1997) *J Biol Chem* 272:32623–32627.
14. Waite JH (2002) *Integr Comp Biol* 42:1172–1180.
15. Zhao H, Robertson NB, Jewhurst SA, Waite JH (2006) *J Biol Chem* 281:11090–11096.
16. Deming TJ (1999) *Curr Opin Chem Biol* 3:100–105.
17. Lee BP, Chao CY, Nunalee FN, Motan E, Shull KR, Messersmith PB (2006) *Macromolecules* 39:1740–1748.
18. Yu ME, Deming TJ (1998) *Macromolecules* 31:4739–4745.
19. Yu ME, Hwang JY, Deming TJ (1999) *J Am Chem Soc* 121:5825–5826.
20. Burzio LA, Waite JH (2000) *Biochemistry* 39:11147–11153.
21. Haemers S, Koper GJM, Frens G (2003) *Biomacromolecules* 4:632–640.
22. Taylor SW, Chase DB, Emptage MH, Nelson MJ, Waite JH (1996) *Inorg Chem* 35:7572–7577.
23. Sever MJ, Weisser JT, Monahan J, Srinivasan S, Wilker JJ (2004) *Angew Chem Int Ed* 43:448–450.
24. Lee H, Scherer NF, Messersmith PB (2006) *Proc Natl Acad Sci USA* 103:12999–13003.
25. Williams T, Marumo K, Waite JH, Henkens RW (1989) *Arch Biochem Biophys* 269:415–422.
26. Taylor SW, Luther GW, Waite JH (1994) *Inorg Chem* 33:5819–5824.
27. Johnson KL, Kendall K, Roberts AD (1971) *Proc R Soc London Ser A* 324:301–313.
28. Kendall K (1995) *Fundamentals of Adhesion and Interfaces* (VSP, Utrecht, The Netherlands), pp 247–260.
29. Autumn K (2006) *Am Sci* 94:124–132.
30. Smeathers JE, Vincent JFV (1979) *J Mollus Stud* 45:219–230.
31. Turner NJ, Murphy MO, Kielty CM, Shuttleworth A, Black RA, Humphries MJ, Walker MG, Canfield AE (2006) *Circulation* 114:820–829.
32. Katsumi A, Orr AW, Tzima E, Schwartz MA (2004) *J Biol Chem* 279:12001–12004.
33. Waite JH (1995) *Methods Enzymol* 258:1–20.
34. Waite JH (1991) *Anal Biochem* 192:429–433.